Almost fluids: nematic elastomers and granular material under shear

2003 J. Phys.: Condens. Matter 15 S47

(http://iopscience.iop.org/0953-8984/15/1/305)

INSTITUTE OF PHYSICS PUBLISHING JOURNAL OF PHYSICS: CONDENSED MATTER

J. Phys.: Condens. Matter **15** (2003) S47–S55 PII: S0953-8984(03)54673-2

Almost fluids: nematic elastomers and granular material under shear

T C Lubensky

Department of Physics and Astronomy, University of Pennsylvania, Philadelphia, PA 19104, USA

E-mail: tom@physics.upenn.edu.

Received 11 October 2002
Published 16 December 2002
Online at stacks.iop.org/JPhysCM/15/S47

Abstract

Two systems that are not fluids but that have properties normally associated with fluids will be discussed: nematic elastomers, which are liquid crystalline rubbers whose shear modulus vanishes because of a spontaneous broken symmetry, and granular materials under flow. Kinetic–hydrodynamic equations for the latter materials will be used to discuss flows in Couette cells and down rough inclined planes.

1. Introduction

Fluids are materials that flow freely and that cannot support a shear stress. True equilibrium fluids have a number of other properties. In the absence of external potentials such as gravity, they are isotropic and spatially homogeneous; their density, pressure, and temperature are spatially uniform. Liquid crystals are materials that lack the rotational isotropy and sometimes the spatial homogeneity of traditional fluids, yet they cannot support a shear stress in all directions and under appropriate conditions, they can flow. Thus, liquid crystals might be termed 'almost fluids', as indeed their name, which is almost an oxymoron, indicates. In this presentation, I will discuss two other materials that are clearly not fluids but that, nonetheless, have at least some properties normally associated with fluids. The materials are nematic elastomers, which are basically rubbers that in their ideal form spontaneously develop the orientational anisotropy of a nematic liquid crystal, and granular materials that are quiescent unless subjected to external shears, in which case they develop flows that one might hope could be described by hydrodynamic equations similar to those used to describe flow in normal fluids.

2. Nematic elastomers

Rubbers or elastomers and gels are random polymeric networks that can support a shear strain. In their usual form, they are macroscopically isotropic and homogeneous, and for small strains, their elastic energy is identical in form to that of an isotropic solid or a glass, but with

a shear modulus that is much smaller than their bulk modules. Rubbers are usually formed by chemically binding, or cross-linking, pairs of polymers in a dense melt of flexible polymers, whereas gels are usually formed by reactions between multifunctional units in a solutions. Gels can undergo enormous volume changes in response to changes in solvent or temperature [1].

Rigid units can be attached to polymers, either along the main chain or as pendants, to produce the same sequence of nematic and smectic liquid crystalline phases that are found in traditional nonpolymeric thermotropic liquid crystals. These liquid crystal polymers can be weakly cross-linked [2] to produce an elastomer that can condense into various liquid crystalline phases upon cooling. The interplay between liquid crystalline order and shear elasticity leads to unusual properties [3, 4] that may lead to interesting applications, from artificial muscles to actuators, for these thermotropic elastomers. These materials have enormous thermoelastic response and can undergo changes in length by as much as 300% in response to changes in temperature of only a few degrees. Equally striking, as I will discuss in more detail below, is the soft elastic response [5] in nematic elastomers that form by spontaneous symmetry breaking from the isotropic elastomer phase: one of the five elastic moduli that normally characterize a uniaxial solid vanishes and the stress required to create finite strains in certain geometries vanishes in the ideal case.

Though most liquid crystalline elastomers prepared to date have been thermotropic, it is also possible [6] to create lyotropic gels by introducing gel-forming agents (e.g., polyacrylamide) in a dispersion of hard rods such as tobacco mosaic viruses. In the absence of a gel, such rods undergo a transition to the nematic phase upon compression [7]. Polyacrylamide gels can undergo enormous changes in volume in response to changes in temperature or solvent [1]. The volume fraction of rods dispersed in a dilute gel can be increased by compressing the gel and a transition to a nematic gel state can be induced.

To describe the unusual elastic properties of nematic elastomers, it is necessary to review some notation. An equilibrium unstretched elastic medium occupies a region of a Euclidean 3-space, which we will call the reference space S_R. Mass points in this medium are indexed by their vector positions $\boldsymbol{x} = (x_1, x_2, x_3) \equiv (x, y, z)$ in S_R, which are their positions in the unstretched medium. When the medium is distorted, the point originally at $\boldsymbol{x}$ is mapped to a new point $\boldsymbol{R}(\boldsymbol{x}) = (R_1(\boldsymbol{x}), R_2(\boldsymbol{x}), R_3(\boldsymbol{x}))$ in Euclidean space. We will refer to the space of points defined by $\boldsymbol{R}$ as the target space S_T. Since there is no distortion when $\boldsymbol{R}(\boldsymbol{x}) = \boldsymbol{x}$, it is useful to introduce the displacement vector $\boldsymbol{u}(\boldsymbol{x})$ that measures the deviation of $\boldsymbol{R}$ from $\boldsymbol{x}$: $\boldsymbol{R}(\boldsymbol{x}) = \boldsymbol{x}+\boldsymbol{u}(\boldsymbol{x})$. Both S_R and S_T are Euclidean, with distances determined by the unit metric: $\mathrm{d}x^2 = \mathrm{d}x_i\,\mathrm{d}x_i$, and $\mathrm{d}R^2 = \mathrm{d}R_i\,\mathrm{d}R_i$, where the Einstein summation convention on repeated indices is understood. Distortions that vary slowly on a scale set by microscopic lengths of the reference material (interparticle separation in a glass, distance between cross-links in an elastomer, etc) are described by the Cauchy deformation tensor,

$$\Lambda_{ij} = \frac{\partial R_i}{\partial x_j} \equiv \partial_j R_i. \tag{1}$$

Throughout this paper, we will often use matrix notation in which $\underline{\underline{M}}$ is the matrix with components M_{ij} and $\underline{\underline{M}}^{\mathrm{T}}$ is the transpose matrix with components M_{ji}.

The energy of the distorted state relative to the undistorted one depends on the familiar nonlinear Lagrangian strain tensor [8],

$$u_{ij} = \tfrac{1}{2}(\Lambda_{ki}\Lambda_{kj} - \delta_{ij}) = \tfrac{1}{2}(\partial_i u_j + \partial_j u_i + \partial_i u_k\,\partial_j u_k), \tag{2}$$

which is symmetric by construction. It is *invariant* (i.e., transforms as a *scalar*) under arbitrary rotations of the *target* space vector $\boldsymbol{R}$, i.e., if R_i is replaced by $R_i' = O_{Tij}R_j$, where O_{Tij} is an arbitrary rotation matrix, u_{ij} does not change. On the other hand, u_{ij} transforms like a rank-2 *tensor* under rotations of the *reference* space, i.e., if $x_i \to x_i' = O^{-1}_{Rij}x_j$, then $\underline{\underline{u}} \to \underline{\underline{O}}_R\underline{\underline{u}}\,\underline{\underline{O}}_R^{-1}$.

The elastic energy of an isotropic medium must be invariant under rotations $\underline{\underline{O}}_R$ in the reference space and rotations $\underline{\underline{O}}_T$ in the target space. Invariance with respect to rotations in the target space is guaranteed by the use of the Lagrangian strain tensor of equation (2). Invariance with respect to rotations in the references space are enforced by including in the energy only combinations of u_{ij} that are rotationally invariant under $\underline{\underline{O}}_R$, i.e., by including only terms of the form $\mathrm{Tr}\,\underline{\underline{u}}^n$. In the spirit of a Landau expansion, we can, therefore, use a model energy of the form

$$f(\underline{\underline{u}}) = \tfrac{1}{2}\lambda(\mathrm{Tr}\,\underline{\underline{u}})^2 + \mu\,\mathrm{Tr}\,\underline{\underline{u}}^2 - C\,\mathrm{Tr}\,\underline{\underline{u}}^3 + D(\mathrm{Tr}\,\underline{\underline{u}}^2)^2 - E\,\mathrm{Tr}\,\underline{\underline{u}}\,\mathrm{Tr}\,\underline{\underline{u}}^2, \tag{3}$$

where λ and μ are the usual Lamé coefficients for an isotropic solid, and C, D, and E are phenomenological constants. Usually, only the second-order terms are included. We, however, are interested in situations in which there is a phase transition from the isotropic phase to an anisotropic phase in which $R_i(\boldsymbol{x}) = R_{0i}(\boldsymbol{x}) = \Lambda_{0ij}x_j$ and there is a nonvanishing anisotropic strain tensor,

$$\underline{\underline{u}}_0 = \tfrac{1}{2}(\underline{\underline{\Lambda}}_0^{\mathrm{T}}\underline{\underline{\Lambda}}_0 - \underline{\underline{\delta}}) = \tfrac{1}{2}\Lambda_{0\perp}^2[(1-\Lambda_{0\perp}^{-2})\underline{\underline{\delta}} + (r-1)\boldsymbol{n}_0\boldsymbol{n}_0], \tag{4}$$

where $\boldsymbol{n}_0$ is the unit vector specifying the direction of stretch. $\Lambda_{0ij} = \Lambda_{0\perp}\delta_{ij} + (\Lambda_{0||} - \Lambda_{0\perp})n_{0i}n_{0j}$ is the equilibrium deformation tensor. The anisotropy of the nematic state can be characterized by the anisotropy ratio $r = \Lambda_{0||}^2/\Lambda_{0\perp}^2$. In incompressible systems, $\det\underline{\underline{\Lambda}}_0 = \Lambda_{0||}\Lambda_{0\perp}^2 = 1$, $\Lambda_{0\perp} = \Lambda_{0||}^{-1/2}$, leading to $r = \Lambda_{0||}^3$. As we will see below, many of the properties of the uniaxial phase depend critically on r.

We wish to explore the elasticity of spontaneously uniaxially ordered nematic elastomers. Distortions of these equilibrium systems can be described by deviations,

$$\delta\underline{\underline{u}} = \underline{\underline{u}} - \underline{\underline{u}}_0 = \tfrac{1}{2}(\underline{\underline{\Lambda}}^{\mathrm{T}}\underline{\underline{\Lambda}} - \underline{\underline{\Lambda}}_0\underline{\underline{\Lambda}}_0), \tag{5}$$

of the strain tensor $\underline{\underline{u}}$ from its new equilibrium value $\underline{\underline{u}}_0$, both measured in the coordinates $\boldsymbol{x}$ of the original isotropic state, S_R. It is, however, more common and convenient to describe these distortions in terms of displacements $\boldsymbol{R}'(\boldsymbol{x}') \equiv \boldsymbol{R}(\boldsymbol{x})$ and strains $\underline{\underline{u}}'(\boldsymbol{x}')$ expressed as functions of the coordinates $\boldsymbol{x}' \equiv \boldsymbol{R}_0(\boldsymbol{x})$ of the new equilibrium stretched state $S'_R \equiv S_T^0$: $\boldsymbol{R}'(\boldsymbol{x}') = \boldsymbol{x}' + \boldsymbol{u}'(\boldsymbol{x}')$ and $\underline{\underline{u}}' = \frac{1}{2}(\underline{\underline{\Lambda}}'^T\underline{\underline{\Lambda}}' - \underline{\underline{\delta}})$, where $\Lambda'_{ij} = \partial R'_i/\partial x'_j$. The deviation $\delta\underline{\underline{u}}$ is directly proportional to $\underline{\underline{u}}'$:

$$\delta\underline{\underline{u}} = \underline{\underline{\Lambda}}_0^{\mathrm{T}}\underline{\underline{u}}'\underline{\underline{\Lambda}}_0. \tag{6}$$

One would normally expect the elastic free energy for strains $\underline{\underline{u}}'$ about the new uniaxial state to have the form of a uniaxial solid [8] characterized by five independent elastic constants. However, the fact that the uniaxial state arose via *spontaneous* symmetry breaking of an isotropic state guarantees that the shear modulus, C_5, measuring the energy of strains in planes containing $\boldsymbol{n}_0$ *must* vanish.

Since the original free energy is invariant under rotations $\underline{\underline{O}}_R$ in S_R and the anisotropy direction $\boldsymbol{n}_0$, which we take to be along the z-axis in S_T, is arbitrary, states characterized by strain $\underline{\underline{O}}_R\underline{\underline{u}}_0\,\underline{\underline{O}}_R^{-1}$ and $\underline{\underline{u}}_0$ must have the same bulk energy. This means that there is no bulk energy cost associated with any strain of the form

$$\underline{\underline{u}}'(\theta) = (\underline{\underline{\Lambda}}_0^{\mathrm{T}})^{-1}(\underline{\underline{O}}_R\underline{\underline{u}}_0\underline{\underline{O}}_R^{-1} - \underline{\underline{u}}_0)\underline{\underline{\Lambda}}_0^{-1}, \tag{7}$$

relative to the uniaxial state characterized by $\underline{\underline{u}}_0$, since it describes a rotation in S_R. It can be shown [4] that this invariance implies that there is no energy cost associated with an infinitesimal strains $u'_{xz} = u'_{zx}$ and $u'_{yz} = u'_{zy}$. Thus, the shear elastic modulus C_5 must identically vanish

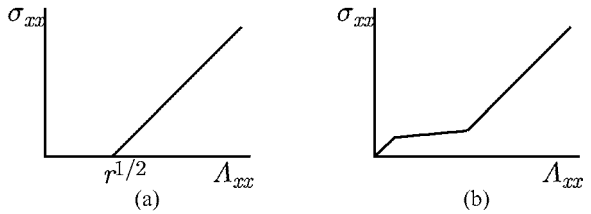

Figure 1. Stress σ_{xx} versus strain Λ_{xx} for an ideal soft nematic elastomer stretched along a direction perpendicular to the direction of initial alignment. The stress is zero up to a critical strain $\Lambda_{xx} = \sqrt{r}$. Beyond that it initially grows linearly from zero.

in a *spontaneously* uniaxial state. Its *harmonic* elastic energy is, therefore, characterized by only four elastic constants and is given by

$$f^N_{\rm uni} = \tfrac{1}{2}C_1 u'^2_{zz} + C_2 u'_{zz}(u'_{xx} + u'_{yy}) + \tfrac{1}{2}C_3(u'_{xx} + u'_{yy})^2 + C_4(u'^2_{xx} + u'^2_{yy} + 2u'^2_{xy}). \tag{8}$$

Because $f^N_{\rm uni}$ contains only harmonic terms in u'_{ij}, it is only invariant with respect to *infinitesimal* rotations in S_R, and terms nonlinear in u'_{ij} must be incorporated in order to encode the full O_R-invariance [10].

There are striking experimental consequences of the existence of zero-energy strains $\underline{\underline{u}}'(\theta)$ given by equation (7) for arbitrary $\underline{\underline{O}}_R$. If a strain $u'_{xx}$is imposed along the x-direction perpendicular to the anisotropy direction, the anisotropy axis can rotate so as to allow the stretch to occur without any energy cost. The result is that no stress is required to produce the strain u'_{xx} until Λ'_{xx} reaches a value of $r^{1/2}$ at which point the anisotropy axis is aligned along x, and further stretching requires a stress. The stress–strain relation for this semi-soft elasticity is shown in figure 1.

Random stresses, inherent in any rubber, produce random orientational fields for the nematic degrees of freedom and make it difficult, if not impossible, to produce a true monodomain sample of a nematic elastomer without the imposition of an aligning stress at the moment of cross-linking. This uniaxial stress breaks the rotational symmetry of the originally isotropic elastomer and gives rise to an extra term $-\sigma_{zz}u_{zz}$ in equation (3). As a result, the nematic state will align along the z-axis, and the nematic state will not exhibit true soft elasticity with the stress–strain curve shown in figure 1(a); rather it will exhibit semi-soft elasticity [9, 10] with a stress–strain curve such as that shown in figure 1(b).

3. Granular flow

Granular materials [11], such as sand and flour, are composed of small grains or particles that are nevertheless so large that, unlike atoms in a liquid or colloidal particles dispersed in a fluid, their centre-of-mass motion due to thermal fluctuations is negligibly small. When confined to containers under gravity, granular materials are essentially quiescent though they may undergo slow rearrangement processes in response to gravitational stress. When subjected to sufficiently large shears, however, they can fluidize and flow. Under flow, granular particles undergo collisions with their neighbours and develop random velocity fluctuations like particles in a fluid. It seems reasonable, therefore, that granular materials under flow might be characterized by a local pressure P and a local granular temperature T, proportional to fluctuations in the velocity, in addition to an average velocity $\boldsymbol{V}$ and that they should, therefore, be described by hydrodynamic equations similar to the Navier–Stokes equations for a fluid even though collisions between particles are inelastic and may have components due to

solid friction. Indeed, there is a considerable body of literature on hydrodynamic theories of granular flow [12].

Here I will describe a hydrodynamic theory [13] designed to treat dense as well as dilute granular materials under flow and use it to describe flow in Couette cells and down a rough inclined plane [14]. Like previous theories, it is based on the Chapman–Enskog kinetic theory of fluids, but it includes a more rapid divergence of the shear viscosity as the close-packing density is approached than would be predicted by that theory. In spite of its limitations, which will be discussed more fully below, this theory predicts velocity and temperature profiles that are in remarkable agreement with shear experiments in Couette geometry [13, 15], and it predicts a purely dynamical jammed-to-flowing transition in chute flow down a plane that also is in remarkably good agreement with detailed simulations [16].

We take the point of view that a flowing granular material behaves locally like a hard-sphere fluid with colliding particles that generate a kinetic pressure P proportional to the temperature. The pressure diverges as the number density n approaches the random-close-packing density n_c, and the free volume available to a given particle vanishes:

$$P = n[1 - (n/n_c)]^{-1}T. \tag{9}$$

This equation of state neglects stresses mediated by the enduring contacts between particles that are responsible for force chains and anisotropies in the pressure. These contacts are certainly important, especially near the static limit and when the gravitational length is smaller than a particle diameter. We will, nonetheless, neglect them for the moment.

In the steady state in a uniform gravitational field $\boldsymbol{g}$, the Navier–Stokes equation for the momentum becomes the force-balance equation for a fluid of mass density $\rho = mn$, where m is the particle mass:

$$\partial_j \sigma_{ij} = -\rho g_i, \tag{10}$$

where $\sigma_{ij} = -P\delta_{ij} + 2\eta\dot{\gamma}_{ij}$ is the stress tensor with η the shear viscosity and $\dot{\gamma}_{ij} = (\partial_i V_j + \partial_j V_i)/2$ is the shear-rate tensor. For simplicity, we will consider only situations in which the velocity is along the x-direction, and there is only spatial variation along y. In this case, the only nonvanishing component of $\dot{\gamma}_{ij}$ is $\dot{\gamma} = \partial_y V_x$, and the temperature equation becomes

$$\partial_y[\lambda(n, T)\,\partial_y T] + [\sigma_{xy}^2/\eta(n/n_c, T)] - \epsilon(n, T)T = 0, \tag{11}$$

where $\lambda(n, T)$ is the thermal conductivity and $\epsilon(n, T)$ is the dissipative coefficient describing irreversible heat loss.

For most applications in normal fluids, the transport coefficients are effectively constants. This is not the case for granular fluids in which the granular temperature goes to zero as the shear rate goes to zero; the dependences of transport coefficients on density and temperature are important. Following earlier work [12], we use the Chapman–Enskog expressions for the thermal conductivity and heat-loss coefficients:

$$\begin{aligned} \lambda(\rho, T) &= [\lambda_0/(m^{1/2}d^2)][1 - (n/n_c)]^{-1}T^{1/2}; \\ \epsilon(\rho, T) &= (\epsilon_0 m^{1/2} n_c/d)[1 - (n/n_c)]^{-1}T^{1/2}, \end{aligned} \tag{12}$$

which diverge as $[1 - (n/n_c)]^{-1}$ as n_c is approached. For η, we deviate from the standard Chapman–Enskog result and allow for a more rapid divergence with n near n_c as simulations [17] and mode-coupling theories [18] suggest:

$$\eta(n/n_c, T) = \eta_0[m^{1/2}/d^2]\phi(n/n_c)T^{1/2}, \tag{13}$$

where $\phi(n/n_c)$ is a function that crosses over from the Chapman–Enskog behaviour of $(1 - n/n_c)^{-1}$ at intermediate and low densities to a more rapid divergence near n_c. For densities near n_c, we take

$$\phi(n/n_c) = A(1 - n/n_c)^{-\beta}, \tag{14}$$

where A is a constant and $\beta > 1$ is an exponent that can be viewed as a phenomenological parameter to be set by experiments and is in the range 1.5–1.75 [13, 15]. In chute flow down an inclined plane, the density can in general pass from low to high, and we use the expression $\phi(x) = [(1 - x)^{\beta-1} + \alpha_0^{\beta-1}/(1 - x)^{\beta}(1 + \alpha_0^{\beta-1})]$, which interpolates smoothly between the low- and high-density limits.

In Couette experiments, granular material is confined between two concentric cylinders and the inner cylinder is spun, thereby generating shear flow that decays as the outer cylinder is approached. If we ignore gravity, then from equation (10), both the pressure P and σ_{xy} are constant, so $\sigma_{xy} = \eta(n/n_c, T)\dot{\gamma} = \text{constant}$. The granular density is generally near the random-close-packing density, and we expect the anomalous form (equation (14)) of the viscosity to apply. In this case, we obtain a power-law relation $\dot{\gamma} \sim T^{\frac{1}{2}(2\beta-1)}$ between shear rate and temperature. Thus, the shear rate is proportional to a power of the temperature. Measurements by Losert *et al* [13] and by Mueth [15] are consistent with this behaviour and yield, respectively, exponents of $\beta = 1.75$ and 1.5.

In the dense regime, the nonlinear heating term in the temperature equation, equation (11), scales as $\sigma_{xy}^2/\eta(n/n_c, T) \sim T^{(2\beta-1)/2}$ and approaches zero more rapidly with T than does the heat-loss term $\epsilon T \sim T^{1/2}$. Thus, as shear rate and temperature decrease with distance from the inner cylinder, the nonlinear heating term eventually becomes small compared to the heat-loss term, and the former can be neglected relative to the latter for distances greater than a crossover length y_w. Thus, for $y > y_w$, the equation for the temperature takes the simple form

$$\partial_y^2 T^{1/2} - \delta^{-2} T^{1/2} = 0, \tag{15}$$

where δ has the dimension of a length and is defined by $\delta^2 = 2\lambda_0/(\epsilon_0 \rho_0 d)$. In the pure Chapman–Enskog theory [12], both the nonlinear heating and the heat-loss terms scale as $T^{1/2}$, and both remain equally important throughout the sample.

Equation (15) can easily be solved for $T^{1/2}$ with the boundary condition that it reach a value of T_0 at $y = y_w$. The result is

$$T^{1/2}(y) = T_0^{1/2} \frac{\cosh[(H - y)/\delta]}{\cosh[(H - y_w)/\delta]}. \tag{16}$$

Experimental data [13, 15] are in excellent agreement with this result. Once the temperature has been found, the velocity $v(y)$ can be obtained by integrating the equation relating $\dot{\gamma} = \partial_y v/2$ to T. Again, the result is in good agreement with experiment.

Granular material on a rough inclined plane will flow for a sufficiently high angle θ of incline relative to the horizontal [19, 20]. Pouliquen [19] recently measured flows down such a plane and found a remarkable phase diagram in which there is no flow for the thickness H of the flowing layer less that a critical value $H_{\text{stop}}(\theta)$ that depends on the tilt angle. For H greater than $H_{\text{stop}}(\theta)$ but not too much greater, there is a steady uniform flow. For larger values of H (or equivalently sufficiently large values of θ at fixed H), flow becomes unsteady and difficult to measure. Detailed simulations reproduce these results with considerable accuracy [16].

Application of the kinetic hydrodynamical equations discussed above is straightforward. Unlike the situation in Couette geometry, gravity is responsible for the flow and cannot be neglected. We introduce dimensionless variables $v = V_x/\sqrt{gd}$, $t = T/(\rho_c g d)$, $\sigma = \sigma_{xy}/(\rho_c g d)$, $p = P/(\rho_c g d)$, take the x-axis to be parallel to the plane and the y-axis normal

to it, and measure distance in units of the particle diameter d. The equations for pressure and temperature are then

$$\frac{\partial}{\partial y} p = -\cos\theta \frac{t}{p+t} \tag{17}$$

$$\partial_y \left(\left(\frac{p+t}{t^{1/2}} \right) \partial_y t \right) + a \frac{\sigma^2}{\phi(\frac{p}{p+t}) t^{1/2}} - bpt^{1/2} = 0, \tag{18}$$

where $p/(p+t) = \rho/\rho_c$ is the reduced density, $a = (\rho_c d^3)^2/(\lambda_0 \eta_0)$ and $b = \epsilon_0 \rho_c d^3/\lambda_0$ are dimensionless constants, σ is related to p according to $\sigma = \tan\theta p + c$, with c an as yet unspecified constant. The parameters appearing in equation (18) are strongly constrained by the complementary experiments performed in the Couette cell [13, 15]. In this case, the velocity and temperature profiles are localized close to the moving boundary over a depth of a few particle diameters. This behaviour is predicted by the hydrodynamic model with a characteristic decay length for the RMS velocity given by $\delta/d = (2/b)^{1/2}$ [13]. Experimentally, δ is of the order of 4–5 particle diameters, yielding $b \simeq 0.1$ (we shall use in the following $b = 0.111$). The exponent β is assumed to have the same value, 1.5–1.75, as in the Couette experiments. The parameter α_0 in $\phi(x)$ is chosen such that the crossover to the anomalous scaling occurs roughly 10% below random close packing. In practice, $\alpha_0 = 0.05$ is adequate. Eventually, a is expected to be of order unity.

The hydrodynamic equations (17) and (18) have to be supplemented by boundary conditions for the velocity and temperature fields at the bottom and top surfaces. As described in [14], we take $\partial_y T = 0$ at both boundaries, $v = 0$ at $y = 0$ and $\sigma = 0$, implying $\partial_y v = -$ at $y = H$. Since, as mentioned above, the effective hydrodynamic boundary $y = H$ is located slightly inside the material, the pressure is not expected to vanish there, and it can be written as $p_0 = y_0 \cos\theta$ (in reduced units) with y_0 a *molecular* distance of the order of the diameter (unity in reduced units). To ensure full consistency with the stress-free boundary for the velocity, we thus write $\sigma = \tan\theta(p - p_0)$ (i.e., fix the constant $c = -\tan\theta p_0$). As emphasized above, this is a molecular effect that disappears in the large-H limit. Moreover, this choice does not affect the existence of the jammed-to-flowing transition to be discussed now.

Numerical solutions to the system of equations (17) and (18) yield a transition between two kinds of behaviour: for a set $\{H, \theta\}$ such that H is below a critical $H_{\rm stop}(\theta)$ curve, only the $T = 0$ solution exists. This corresponds to a 'jammed' state, which stays at rest. Above this critical value, nonzero solutions for the temperature which correspond to a flowing regime do exist. Figure 2(a) shows the boundary between the two regimes, denoted as $H_{\rm stop}(\theta)$ as in [19]. This curve is in qualitative agreement with the experimental results of [19] and simulations of [16]. Thus the hydrodynamic model is able to generate a finite critical angle below which no flow occurs. Within the model, the origin of this behaviour is simply the balance between the 'viscous heating', which generates fluctuations, and dissipation, which tends to inhibit the flow. The transition is thus purely dynamical: a jammed state occurs for low angles/thicknesses because fluctuations are insufficient to allow flow.

Above $H_{\rm stop}(\theta)$, more than one solution can be found for some sets of parameters $\{H, \theta\}$. However, a linear stability analysis of the hydrodynamic equation for the temperature shows that only the nonzero solution with the largest value of $T(H)$ is dynamically stable. On the other hand, the $T = 0$ solution is always linearly stable, but becomes unstable against larger 'kicks' in the temperature. It is important to note that there is a solution to the hydrodynamic equations for any set of H and θ above the boundary $H_{\rm stop}(\theta)$, as is found experimentally. This is in contrast to other approaches where for a given θ a *single* flowing thickness H is selected [21]. In the flowing regime, we obtain temperature and density profiles; those for $H = 40$ are plotted in figure 2(b).

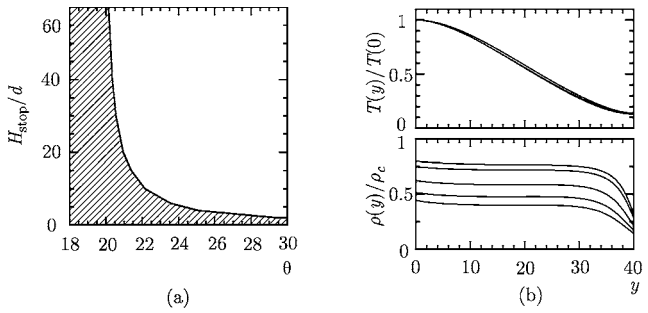

Figure 2. (a) The phase diagram for the jammed-to-flowing transition in a gravity-driven granular material as obtained from the resolution of the hydrodynamic equations (17) and (18). (b) Top: normalized temperature profiles for $H = 40$, $\theta = 20.55°$, $20.90°$, $21.50°$, $22.50°$. Bottom: normalized density profiles for $H = 40$, $\theta = 20.55°$, $20.90°$, $22.50°$, $24.50°$, $26.50°$ from top to bottom. The parameters used are $a = 1.3$, $b = 0.111$, $\alpha_0 = 0.05$, $y_0 = 0.5$.

The results for both the density and temperature are in qualitative agreement with the simulations of [16]. In particular, the density profile is almost constant in the middle of the sample, with a large drop at the top surface, as found numerically. In the simulations, however, the plateau in the density is flatter than ours. Since $\rho(z)/\rho_c$ is always considerably less than 1, the thermal pressure of our model has no trouble supporting the weight of grains. Pressure from enduring contracts does, however, appear to be important in simulations [16, 22] and experiments.

As already mentioned, the kinetic–hydrodynamic theory presented here does not explicitly include nonthermal stresses due to enduring contacts between particles. These contacts are induced by gravitational or other forces tending to compress the material. Indeed, in typical granular experiments, the thermal gravitational length $\lambda_g = T/mg$ is much less than the diameter of a particle. In the experiments of [13], $\lambda_g/d < 10^{-3}$, implying that the density must be tuned to within less than 10^{-3} of n_c in order for thermal pressure alone to support the weight of even one layer of particles[1]. This is clearly not the case, and the hard-sphere thermal equation of state cannot be used to describe the entire Couette column. Why then do the equations here do such a good job of describing the experiments in [13] and [15]? A possible explanation is that these experiments only measure properties of either the topmost or bottom-most layer of particles and that our equations correctly capture the dynamics of these layers. Indeed data from experiments on 2D layers agree well with our theory [23]. It seems likely that the anomalous divergence of the viscosity is associated with dynamic force chains, which are present in both 2D and 3D systems. Gravity plays a similarly important role in experiments and simulations on flow down inclined planes. Out theory, however, produces an $H_{\rm stop}(\theta)$ curve in good agreement with both in a regime in which ρ/ρ_c (see figure 2) is not abnormally close to one and thermal pressure is clearly able to support the material weight.

These considerations raise a number of interesting questions that deserve further study. Would Couette experiments on granular materials in a microgravity environment yield results similar to those obtained on Earth? Would their detailed behaviour be well described by our kinetic–hydrodynamic theory, which is best suited for λ_g/d large? How do the properties of granular flow down an inclined plane change as λ_d is increased? How should a hard-sphere gas be described when λ_g/d becomes of order one or less? Is it even well defined? There is clearly much more to be learned about the flow of granular materials.

[1] The author is grateful to Greg Voth for bringing this fact to his attention.

Acknowledgments

Many collaborators contributed to this work, though they are not responsible for this manuscript. They include Ranjan Mukhopadhyay, Leo Radzihovsky, Xiangjun Xing, Wolfgang Losert, Jerry Gollub, Lyderic Bocquet, Andy Lau, and David Lacoste. This work was supported in part by the NSF under Grant DMR 00-96532 and by MRSEC Grant DMR 00-799909.

References

[1] Tanaka T 1977 *Phys. Rev. Lett.* **38** 771
Tanaka T 1978 *Phys. Rev. Lett.* **40** 820
[2] Finkelmann H, Koch H J and Rehage G 1981 *Macromol. Chem. Rapid Commun.* **2** 317
[3] de Gennes P G 1980 *Liquid Crystals of One- and Two-Dimensional Order* ed W Helfrich and G Heppke (New York: Springer) p 231
Warner M and Terentjev E M 1996 *Prog. Polym. Sci.* **21** 853–91
[4] Lubensky T C, Mukhopadhyay R, Radzihovsky L and Xing X 2002 *Phys. Rev.* E
[5] Blandon P, Terentjev E M and Warner M 1994 *J. Physique* II **4** 75
Golubović L and Lubensky T C 1989 *Phys. Rev. Lett.* **63** 1082–5
Olmsted P D 1994 *J. Physique* II **4** 2215–30
[6] Lacoste D, Lau A and Lubensky T C 2002 *Europhys. J.* E **8** 403–11
Engle A, Alsayed A, Zhand J, Dogic Z, Dalheimer P, Discher D and Yodh A G unpublished
[7] Onsager L 1949 *Ann. N Y Acad. Sci.* **51** 627
Dogic Z and Fraden S 2001 *Phil. Trans. R. Soc.* A **359** 997
[8] Landau L D and Lifshitz E M 1986 *Theory of Elasticity* 3rd edn (New York: Pergamon)
[9] Finkelmann H, Kundler I, Terentjev E M and Warner M 1997 *J. Physique* II **7** 1059
Warner M 1999 *J. Mech. Phys. Solids* **47** 1355
[10] Lubensky T C and Mukhopadhyay R unpublished
[11] Clement E 1999 *Curr. Opin. Colloid Interface Sci.* **4** 294
Behringer R P *et al* 1999 *Physica* D **133** 1
Mueth D M *et al* 2000 *Nature* **406** 385
Jaeger H M, Nagel S R and Behringer R P 1996 *Rev. Mod. Phys.* **68** 1259
[12] Jenkins J T and Savage S B 1983 *J. Fluid Mech.* **130** 187
Haft P K 1983 *J. Fluid Mech.* **134** 401
Jenkins J T 1994 *Appl. Mech. Rev.* **47** 240
[13] Losert W, Bocquet L, Lubensky T C and Gollub J P 2000 *Phys. Rev. Lett.* **85** 1428
Bocquet L *et al* 2002 *Phys. Rev.* E **65** 1307
[14] Bocquet L, Errami J and Lubensky T C 2001 *Preprint* cond-mat/0112072
[15] Müth D 2001 *Preprint* cond-mat/0103557
[16] Ertaz D *et al* 2001 *Europhys. Lett.* **56** 214
Silbert L *et al* 2001 *Phys. Rev.* E **64** 051302
[17] Alder B J, Gass D and Wainwright T 1970 *J. Chem. Phys.* **53** 3813
[18] Leutheusser E 1982 *J. Phys. C: Solid State Phys.* **15** 2801
Leutheusser E 1982 *J. Phys. C: Solid State Phys.* **15** 2826
[19] Pouliquen O 1999 *Phys. Fluids* **11** 542
[20] Daerr A and Douady S 1999 *Nature* **399** 241
Azanza E, Chevoir F and Moucheron P 1999 *J. Fluid Mech.* **400** 199
Ancey C 2001 *Phys. Rev.* **65** 011304
[21] Johnson P C, Nott P and Jackson R 1991 *J. Fluid Mech.* **210** 501
Anderson K G and Jackson R 1992 *J. Fluid Mech.* **241** 145
[22] Ertras D and Thomas C H 2002 *Preprint* cond-mat/0206046
[23] Howell D, Behringer R P and Veje C 1999 *Phys. Rev. Lett.* **82** 5241
(Bocquet L unpublished analysis of data; unpublished fluctuation data provided by Howell)